

Tools for Studying Low-Mass Dark Matter at Neutrino Detectors

Jason Kumar, John G. Learned, and Stefanie Smith

*Department of Physics and Astronomy,
University of Hawaii, Honolulu, HI 96822 USA*

Katherine Richardson

*Department of Physics and Astronomy,
University of New Mexico, Albuquerque, NM 87131 USA*

Abstract

We determine the neutrino spectra arising from low-mass ($4 - 10$ GeV) dark matter annihilating in the sun. We also determine the low-mass dark matter capture rates (element by element in the sun), assuming dark matter interacts either through elastic contact interactions, elastic long-range interactions, or inelastic contact interactions. These are the non-detector-specific data needed for determining the sensitivity of a neutrino detector to dark matter annihilating in the sun. As an application, we estimate the sensitivity of a one kiloton liquid scintillation neutrino detector (such as KamLAND) and LBNE (LAr-based) to low-mass dark matter with long-range interactions and compare this to the expected CDMS sensitivity. It is found that KamLAND's sensitivity can exceed that obtainable from the current CDMS data set by up to two orders of magnitude.

I. INTRODUCTION

There has been great recent interest in low-mass dark matter ($m_X \sim \mathcal{O}(10)$ GeV) as a possible explanation for the event rates observed at the DAMA [1], CoGeNT [2] and CRESST [3] experiments. However, negative results from XENON10/100 [4, 5] and CDMS [6–8] have created some tension with these positive signals. There has been much discussion in the literature regarding experimental issues with all of this data, but the explanation is far from clear [9–17]. It is important to find new tests of this data, particularly tests that do not suffer from the same difficulties as direct detection experiments at low recoil energy. Collider, gamma-ray, and anti-proton flux search strategies have been employed for this purpose [18–27].

A promising avenue for cross-checking the low-mass direct detection data is with neutrino detectors [28–33], which search for the flux of neutrinos arising from dark matter annihilation in the core of the sun. Dark matter is captured by the sun via scattering off solar nuclei. If the sun is in equilibrium, then the dark matter capture rate determines the dark matter annihilation rate. The neutrino flux thus constrains the dark matter-nucleus scattering cross-section, and allows neutrino detectors to cross-check direct detection experiments without some of the particle physics and astrophysics uncertainties that plague other types of indirect detection searches. Moreover, the $\mathcal{O}(\text{GeV})$ neutrinos produced from the annihilation of low-mass dark matter are easily distinguishable at water Cherenkov, liquid argon or liquid scintillator-based neutrino detectors.

In order to determine the event rate expected at a neutrino detector, one must calculate the rate at which dark matter is captured by the sun due to scattering and the neutrino spectrum arising from the decay of the dark matter annihilation products. Numerical packages such as DarkSUSY [35] are commonly used for obtaining these rates, which are determined from numerical simulations. However, the required simulations have not been run for masses less than 10 GeV. Moreover, the capture rate has only been calculated assuming that dark matter scatters elastically via a contact interaction. Recent models for reconciling the low-mass direct detection data have included the possibility of dark matter scattering via long-range forces [36, 61, 62], inelastic scattering [39–44], and dark matter interactions which are isospin-violating [30, 39, 45–47]. To determine the sensitivity of neutrino detectors to these models, new capture rate calculations must be performed.

In this work, we calculate the required neutrino spectra and capture rates for low-mass dark matter in the sun. We not only consider the capture rate for elastic contact scattering, but also for inelastic dark matter and for models in which the dark matter-nucleon interaction is mediated by a low-mass particle. We also determine the regions of parameter-space of these models for which dark matter in the sun is in equilibrium.

As an application of these techniques, we consider the sensitivity of a 1 kT liquid scintillation detector with 2135 live days of data (roughly the same exposure as KamLAND) to dark matter with long-range interactions. We find that the sensitivity of neutrino detectors to dark matter with long-range interactions is enhanced, because typical scatters off low-mass targets (such as the hydrogen and helium in the sun) involve small momentum transfers, yielding enhanced scattering cross-sections in models where the mediating particles are light. This implies the existence of an entire class of dark matter models for which current neutrino experiments can provide the leading sensitivity.

In section II, we review the general formalism for dark matter searches using neutrino detectors. In section III, we describe the details of the computation of the neutrino spec-

trum arising from the annihilation of low-mass dark matter. In section IV, we describe the calculation of the dark matter capture rate in the sun, assuming dark matter with either elastic contact interactions, elastic long-range interactions, or inelastic contact interactions. In section V, we describe the range of circumstances under which low-mass dark matter is in equilibrium in the sun. In section VI, as an example, we apply these techniques to determine the sensitivity of a 1 kT LS neutrino detector to low-mass dark matter with long-range interactions. We conclude in section VII.

II. OVERVIEW OF DARK MATTER DETECTION VIA NEUTRINOS

The rate of charged lepton events at a neutrino detector can be written as

$$R = \frac{\Gamma_A}{4\pi d^2} \int_0^1 dz \sum_{f, \nu_i} B_f \frac{dN_{f, \nu_i}}{dz} \int dV \sigma_{\nu_i-N}(z) \times \eta(r) \times \epsilon(r, z), \quad (1)$$

where $d \sim 1$ AU is the earth-sun distance, $z = E_\nu/m_X$, η is the nucleon number density of the detector (including the earth around the detector, in the case of a search for throughgoing muons), and ϵ is the efficiency for a neutrino charged-current interaction to produce a charged lepton which will pass the detector analysis cuts. B_f is the branching fraction to each dark matter annihilation product f , and $dN_{f, \nu_i}/dz$ is the differential neutrino spectrum per annihilation to each final state, for each (anti-)neutrino flavor. Γ_A is the total dark matter annihilation rate, and σ_{ν_i-N} is the (anti-)neutrino-nucleon scattering cross-section. For dark matter in the 4 – 10 GeV range, most of the charged leptons produced in a reasonably-sized detector will be fully-contained, with the vertex where the lepton is produced and the end of the track both within the fiducial volume of the detector. As a result, we will focus on fully-contained lepton events.

The quantities η and ϵ are specific to the geometry and construction of the detector. For $1 \text{ GeV} < E_\nu < 1 \text{ TeV}$, the σ_{ν_i-N} can be approximated as [48]

$$\begin{aligned} \sigma_{\nu-p} &\simeq 4.51 \times 10^{-3} \times z (m_X / \text{GeV}) \text{ pb}, \\ \sigma_{\nu-n} &\simeq 8.81 \times 10^{-3} \times z (m_X / \text{GeV}) \text{ pb}, \\ \sigma_{\bar{\nu}-p} &\simeq 3.99 \times 10^{-3} \times z (m_X / \text{GeV}) \text{ pb}, \\ \sigma_{\bar{\nu}-n} &\simeq 2.50 \times 10^{-3} \times z (m_X / \text{GeV}) \text{ pb}. \end{aligned} \quad (2)$$

The two remaining quantities we will need to compute are Γ_A and dN_f/dz .

For a search for fully-contained charged leptons, we can then write

$$R = \frac{\Gamma_A}{4\pi d^2} \times \int_0^1 dz \sum_{f, \nu_i} B_f \frac{dN_{f, \nu_i}}{dz} z \times A_{eff.}(z), \quad (3)$$

where

$$A_{eff.}(z) = \sigma_{\nu_i-N}(E_\nu = m_X) \int dV \eta(r) \times \epsilon(r, z). \quad (4)$$

All detector-specific information is encoded in the effective area, $A_{eff.}(z)$.

If $m_X \lesssim 4 \text{ GeV}$, the effect of dark matter evaporation can be important [28, 34]. In that case, dark matter in the sun's core is significantly depleted by evaporation, and the

total annihilation rate is relatively small, implying that constraints on dark matter from the neutrino flux will be weak. We focus on the regime $m_X \geq 4$ GeV, for which dark matter in the sun can only be depleted through annihilation. If the sun is in equilibrium, we then find that Γ_A is related to the dark matter capture rate, Γ_C , by the relation $\Gamma_C = 2\Gamma_A$. Since Γ_C is determined by the dark matter-nucleus scattering cross-section, the above relation allows one to translate neutrino flux bounds into bounds on the dark matter-nucleon scattering cross-section.

III. NEUTRINO SPECTRA

For low-mass dark matter ($m_X \leq 20$ GeV), the only dark matter annihilation products relevant for neutrino searches are heavy quarks (b , c), τ , $\nu_{e,\mu,\tau}$ and the gluon (g). Muons and light quarks (u , d and s) will tend to stop within the sun before they decay [49]. The resulting neutrinos are thus very soft (though they also can potentially be used for dark matter searches [50]).

We have calculated the differential neutrino spectrum per annihilation for the relevant channels using the DarkSUSY/WimpSim/NuSigma/Pythia [35, 51, 52] package. Numerical simulations were run on the Hawaii Open Supercomputing Center (HOSC) computing cluster. 10^7 annihilations were simulated for each annihilation channel and dark matter mass in the range 4 – 10 GeV (in increments of 2 GeV). Representative spectra are plotted in Appendix A, and all of the original data files are available at <http://www.phys.hawaii.edu/~superk/post/spectrum>. We present the neutrino spectrum at a distance 1 AU from the sun, including the effects of hadronization and decay of the annihilation products at injection, matter effects as the neutrinos propagate through the sun (including tau-regeneration) and vacuum oscillations. The neutrino oscillation parameters were chosen to be

$$\begin{aligned}\theta_{12} &= 33.2^\circ, \\ \theta_{23} &= 45^\circ, \\ \Delta m_{21}^2 &= 8.1 \times 10^{-5} \text{ eV}^2, \\ \Delta m_{32}^2 &= 2.2 \times 10^{-3} \text{ eV}^2, \\ \theta_{13} &= 10^\circ,\end{aligned}\tag{5}$$

assuming a normal hierarchy. This choice is consistent with recent exciting data from the Daya Bay experiment [53] indicating $\theta_{13} \sim 9^\circ$. Data files for the choice $\theta_{13} = 0^\circ$ are also available online. For this choice, the change in the neutrino spectrum is relatively small unless dark matter annihilates directly to neutrinos in a flavor-dependent way.

In the case where dark matter annihilates to b -quarks, annihilation can only proceed if the dark matter mass is larger than the mass of the b -hadron which is produced. Moreover, a b -quark will lose $\sim 27\%$ of its energy during hadronization [49, 54]. Thus, the neutrino spectrum arising from annihilation to b -quarks is simulated only for $m_X \geq 6$ GeV. In the case where dark matter annihilates to $\tau\bar{\tau}$, the neutrino spectrum has been computed by averaging over helicities. Some dark matter candidates will preferentially decay to certain helicities, which can have a significant effect on the injected neutrino spectrum [55].

The neutrino spectrum at 1 AU is equivalent to the spectrum of downward-going neutrinos at the detector, averaged over the year. This spectrum determines the rate of downward going fully-contained charged leptons. In the case where the charged lepton is upward going

through the earth, one should also include oscillation and matter effects as the neutrinos pass through the earth. These effects depend on the location of the detector and can be determined by inputting the neutrino spectrum at 1 AU into the “WimpEvent” program, with the location of the detector specified.

IV. CAPTURE RATE

The capture rate can be computed following the analysis of [56], and we follow that notation. A dark matter particle in the halo has velocity u , given by a distribution $f(u)$ obeying $\int du f(u) = \eta_X$. Here, η_X is the dark matter number density in the halo. When a dark matter particle is at distance r from the core of the sun, it will have velocity $w = \sqrt{u^2 + v^2}$, where $v(r)$ is the escape velocity from the sun at radius r . Thus, a dark matter-nucleus scatter will result in dark matter capture if the dark matter scatters from velocity w to a velocity $\leq v$.

More generally, however, 3-body interactions can drastically affect the capture rate. As a conservative estimate, one can choose to count as “captured” only dark matter particles which are kinematically constrained to orbits with maximum radius r_0 , often taken to be the radius of Jupiter’s orbit. The velocity to escape from position $r < r_0$ within the sun to radius r_0 is denoted by $v_e(r)$, and is given by the relation $v_e(r)^2 = v(r)^2 - v(r_0)^2$.

The rate for dark matter to be captured in any differential solar volume by scattering off an element with atomic number Z can then be written as

$$\frac{dC_Z}{dV} = \int_{u_{min}}^{u_{max}} du \frac{f(u)}{u} w \Omega_v^-(w), \quad (6)$$

where $u_{min,max}$ are the minimum/maximum dark matter velocities in the halo such that a nuclear scatter at position r resulting in dark matter capture is kinematically possible. $\Omega_v^-(w)$ is the rate per unit time at which a dark matter particle with velocity w will scatter to velocity $< v_e(r)$, and is given by the expression

$$\Omega_v^-(w) = \eta_\odot w \int_{E_{min}}^{E_{max}} dE_R \frac{d\sigma^{Z,A}}{dE_R}, \quad (7)$$

where η_\odot is the number density of the sun, E_{min} is the minimum recoil energy needed for capture, and E_{max} is the maximum recoil energy that is kinematically allowed. $d\sigma^{Z,A}/dE_R$ is the differential cross-section for dark matter to scatter off a nucleus with Z protons and A nucleons.

For any dark matter model, the quantities that must be known to compute the capture rate are $d\sigma^{Z,A}/dE_R$, $E_{min,max}$, and $u_{min,max}$. Given these quantities, we can compute the capture rate numerically using the DarkSUSY code (appropriately modified), with its standard assumptions about solar composition.

A. Elastic Contact Interactions

The most commonly used assumption is that dark matter interacts with nuclei via elastic, isospin-invariant, contact interactions. In this case, we have

$$\begin{aligned}
E_{min} &= \frac{1}{2}m_X (u^2 + v(r_0)^2), \\
E_{max} &= \frac{\mu}{\mu_+^2} \left(\frac{1}{2}m_X w^2 \right), \\
\frac{d\sigma^{Z,A}}{dE_R} &= \frac{\sigma^p}{E_{max}} \left[\frac{(m_X + m_p)^2 m_A^2}{(m_X + m_A)^2 m_p^2} \right] \left[Z + \frac{f_n}{f_p}(A - Z) \right]^2 |F_A(E_R)|^2, \\
u_{max}^2 &= \frac{\mu}{\mu_-^2} \left(v^2 - \frac{\mu_+^2}{\mu} v(r_0)^2 \right), \\
u_{min} &= 0,
\end{aligned} \tag{8}$$

where $\mu \equiv m_X/m_A$ and $\mu_{\pm} \equiv (\mu \pm 1)/2$. $f_{p,n}$ are the relative strengths of dark matter coupling to protons and neutrons, respectively. σ^p is the dark matter-proton scattering cross-section, and $F_A(E_R)$ is the nuclear form factor. To match the assumptions used in DarkSUSY, we will assume a Gaussian form factor $|F_A(E_R)|^2 = \exp[-E_R/E_0]$, where $E_0 = 3\hbar^2/2m_A R_A^2$. $R_A = [0.3 + 0.91(m_A/\text{GeV})^{1/3}]$ fm is taken as the nuclear radius.

Following default assumptions in DarkSUSY [35, 56], we have assumed a Maxwell-Boltzmann velocity distribution for dark matter in the Galactic halo of the form

$$f_{halo}(u) = \eta_X \frac{4}{\sqrt{\pi}} \left(\frac{3}{2} \right)^{\frac{3}{2}} \frac{u^2}{\bar{v}^3} e^{-3u^2/2\bar{v}^2}, \tag{9}$$

where \bar{v} is the three-dimensional velocity dispersion, which we have set to $\bar{v} = 270$ km/s. This velocity distribution is truncated at the galactic escape velocity, v_{esc} . The velocity distribution seen by an observer moving through the halo with velocity v_* is then

$$\begin{aligned}
f(u) &= \frac{f_{halo}(u)}{2} e^{-3v_*^2/2\bar{v}^2} \frac{\bar{v}^2}{3uv_*} \left[\exp\left(\frac{3uv_*}{\bar{v}^2} \cos \theta_{max}\right) - \exp\left(\frac{3uv_*}{\bar{v}^2} \cos \theta_{min}\right) \right] \\
&\quad \times \theta(v_* + v_{esc} - u),
\end{aligned} \tag{10}$$

where

$$\begin{aligned}
\cos \theta_{max} &= 1, \\
\cos \theta_{min} &= \max \left[-1, \frac{u^2 - (v_{esc}^2 - v_*^2)}{2uv_*} \right].
\end{aligned} \tag{11}$$

The step function imposes the condition that $f(u) = 0$ for $u > v_* + v_{esc}$. If we ignore the truncation at the galactic escape velocity, this reduces to the expression

$$f(u) = f_{halo}(u) e^{-3v_*^2/2\bar{v}^2} \frac{\bar{v}^2}{3uv_*} \sinh\left(\frac{3uv_*}{\bar{v}^2}\right). \tag{12}$$

We take $v_* = 220$ km/s to be the velocity of the sun through the halo.

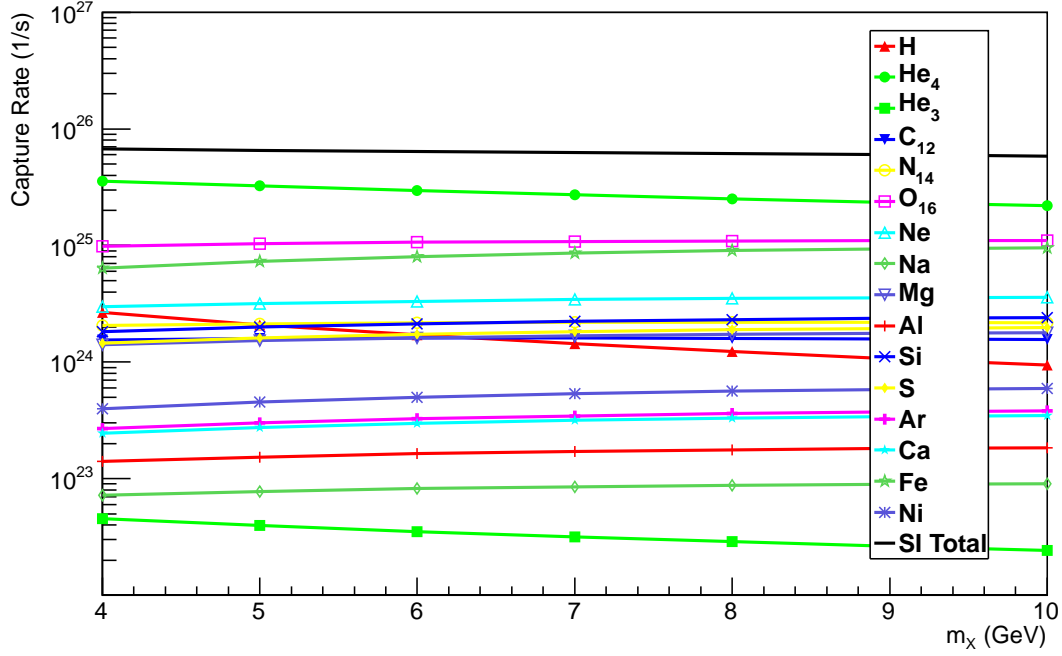


FIG. 1: Solar dark matter capture rates for various elements in the sun, assuming isospin-invariant elastic contact interactions with $\sigma^p = 10^{-4}$ pb.

For isospin-invariant interactions, one assumes $f_n/f_p = 1$. For isospin-violating dark matter, the capture rate from scattering by each element is scaled by a factor $[Z + (f_n/f_p)(A - Z)]^2/A^2$. To facilitate this rescaling in the case of generic isospin-violating interactions, we plot the capture rate for each of the main elements in the sun separately.

We have plotted in fig. 1 the capture rates for elastic contact interactions if one requires dark matter to be captured to within the radius of Jupiter's orbit. If the presence of Jupiter is neglected, capture rates change by less than 1% in the case of elastic contact interactions.

B. Elastic Long-Range Interactions

If dark matter interacts with nuclei via long-range interactions (or, equivalently, via a t -channel interaction with a mediator with a mass much smaller than the momentum transfer), then the differential scattering cross-section will have a different form. The quantum matrix element scales as $\mathcal{M} \propto 1/(q^2 - M_*^2)$ where M_* is the mass of the mediating particle and q is the momentum transfer; for $M_*^2 \ll q^2$, the differential cross-section scales as q^{-4} . For such a model, it would not make sense to parameterize the differential scattering cross-section in terms of σ_p since, as with Rutherford scattering, the total cross-section is infinite. We may instead write

$$\frac{d\sigma^{Z,A}}{dE_R} = C \frac{4\pi\alpha^2\mu_p^2}{m_A^2 E_R^2 E_{max}} \left[\frac{(m_X + m_p)^2}{(m_X + m_A)^2} \frac{m_A^2}{m_p^2} \right] \left[Z + \frac{f_n}{f_p}(A - Z) \right]^2 |F_A(E_R)|^2, \quad (13)$$

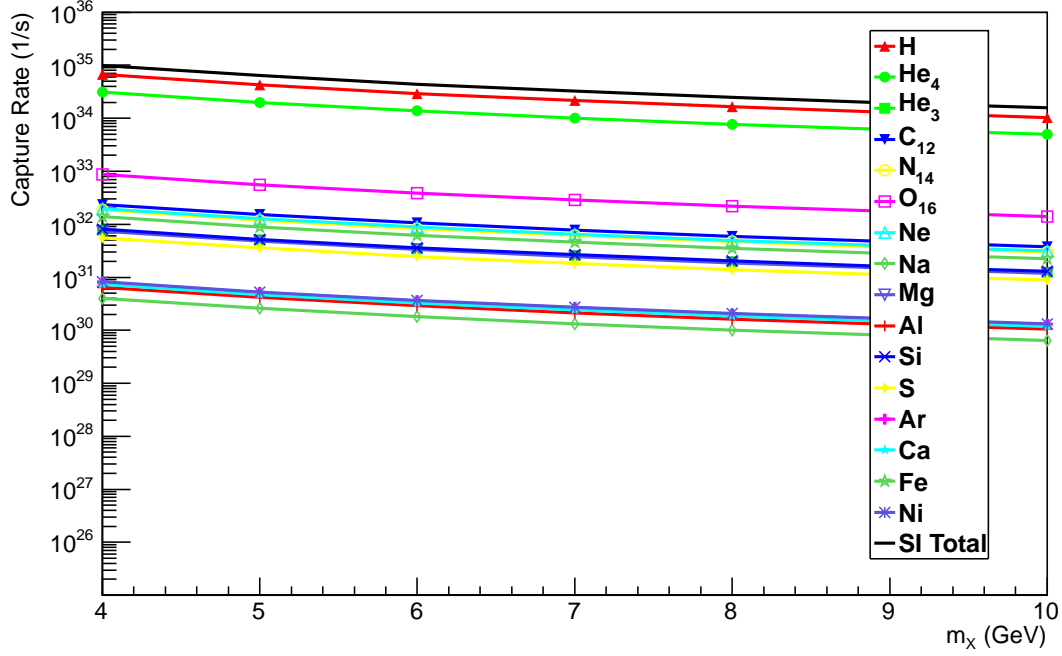


FIG. 2: Solar dark matter capture rates for various elements in the sun, assuming isospin-invariant elastic long-range interactions (as in eq. 13) with $C = 10^{-10}$. Captured dark matter is required to be confined within the orbit of Jupiter.

where $\mu_p = m_X m_p / (m_X + m_p)$ is the dark matter-proton reduced mass. C is a constant which defines the size of the differential scattering cross-section in terms of the proton charge; if $g_{X,p}$ are the strengths with which the mediator couples to the dark matter and a proton, respectively, then $C = g_X^2 g_p^2 / e^4$. Using the Gaussian form factor defined above, the integrated differential scattering cross-section takes the simple form

$$\int_{E_{min}}^{E_{max}} dE_R \frac{d\sigma^{Z,A}}{dE_R} = C \frac{4\pi\alpha^2 \mu_p^2}{m_A^2 E_{max}} \left[\frac{(m_X + m_p)^2}{(m_X + m_A)^2} \frac{m_A^2}{m_p^2} \right] \left[Z + \frac{f_n}{f_p} (A - Z) \right]^2 \times \left[\frac{e^{-\frac{E_{min}}{E_0}}}{E_{min}} - \frac{e^{-\frac{E_{max}}{E_0}}}{E_{max}} + \frac{Ei(-E_{min}/E_0)}{E_0} - \frac{Ei(-E_{max}/E_0)}{E_0} \right]. \quad (14)$$

The kinematics of the scattering process are the same as in the case of an elastic contact interaction, and thus $E_{min,max}$ and $u_{min,max}$ are the same as in equation (8). The capture rates for dark matter with long-range interactions are plotted in fig. 2 (for $m_X = 4 - 10$ GeV) and fig. 3 (for $m_X = 10 - 1000$ GeV), again assuming that captured dark matter must be confined to an orbit inside Jupiter's.

One should note that, in the case of long-range interactions, it is necessary to assume that captured dark matter be confined to an orbit within some finite radius r_0 ; without this assumption, the capture rate would be infinite. The origin of this divergence is easily understood to arise from the low-velocity tail of the Maxwell-Boltzmann velocity distribution. Near $u = 0$, dark matter far from the sun has a very small kinetic energy. As a result, even scattering interactions yielding very small recoil energies can result in a dark matter particle

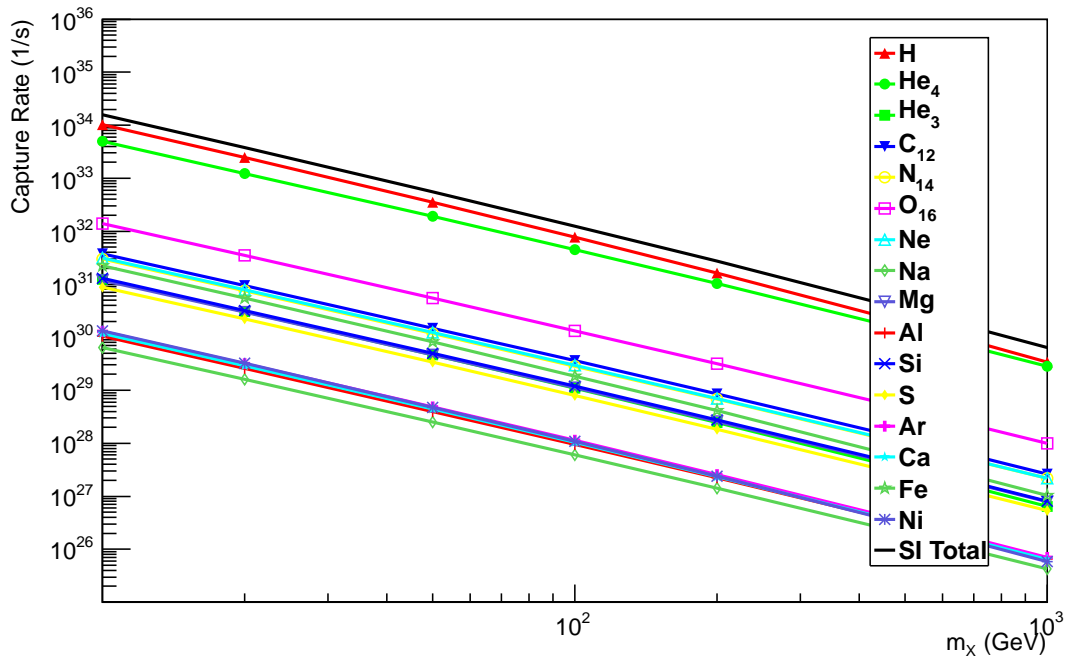


FIG. 3: Solar dark matter capture rates for various elements in the sun, assuming isospin-invariant elastic long-range interactions (as in eq. 13) with $C = 10^{-10}$. Captured dark matter is required to be confined within the orbit of Jupiter. Plotted for dark matter with mass in the range $10 - 1000$ GeV.

being captured, (i. e., having negative total energy). Since the differential scattering cross-section diverges at small recoil energy, the total capture rate diverges. This simply reflects the fact that it is not physically sensible to think of dark matter as captured if confined to an orbit of very large radius. It is most sensible to count as captured only dark matter confined to orbits that lie within Jupiter's orbit.

Note that we are not including the possibility of capture due to multiple scattering. For many models, these effects can significantly enhance the dark matter capture rate, especially in the case of long-range interactions. The dark matter capture rate may be much larger if dark matter scattering exhibits Sommerfeld enhancement. But this depends on the details of the model, including the nature of dark matter interactions with electrons and possible 3-body effects. These issues may be relevant for specific models but are beyond the scope of this work.

C. Inelastic Contact Interactions

One may also consider the case where dark matter scatters inelastically off nuclei, via the process $XA \rightarrow X'A$. We will consider the case with $\delta m_X = m_{X'} - m_X \geq 0$. In this case, the scattering matrix element will only change by subleading $\mathcal{O}(\delta m_X/m_X)$ terms, but the kinematics of the scattering process can change dramatically. It is easiest to consider this process in the center-of-mass frame. We then find $p_i^2 - p_f^2 \approx 2m_r\delta m_X$, where $m_r = m_X m_A / (m_X + m_A)$ is the reduced mass, and $p_i = m_r w$ and p_f are the spatial momenta of the incoming X and outgoing X' , respectively, in the center-of-mass frame. The phase

space factor of the differential scattering cross-section is directly proportional to the outgoing momenta.

Again, it is not appropriate to express the dark matter-nucleus inelastic scattering cross-section in terms of the dark matter-proton scattering cross-section, since there exist kinematic regions where dark matter-proton inelastic scattering is impossible, though dark matter can scatter off other nuclei. Using the fact that the recoil energy can be written as $E_R = (2m_A)^{-1}(p_i^2 + p_f^2 - 2p_i p_f \cos \theta_{cm})$, we can write

$$\frac{d\sigma^{Z,A}}{dE_R} = \frac{m_A I}{32\pi w^2} \left[Z + \frac{f_n}{f_p}(A - Z) \right]^2 |F_A(E_R)|^2, \quad (15)$$

where $m_X^2 m_A^2 [Z + (A - Z)(f_n/f_p)]^2 |F_A(E_R)|^2 \times I$ is the squared dark matter-nucleus matrix element (summed over final spins and averaged over initial spins). I is roughly constant for different elements (up to $\mathcal{O}(\delta m_X/m_X)$ corrections), so it makes sense to present bounds on inelastic dark matter in terms of this quantity. We also find

$$E_{max} = \frac{m_r^2 w^2}{m_A} \left(1 - \frac{\delta m_X}{m_r w^2} + \sqrt{1 - 2 \frac{\delta m_X}{m_r w^2}} \right). \quad (16)$$

Similarly, we find

$$E_{min} = \max \left[\frac{m_r^2 w^2}{m_A} \left(1 - \frac{\delta m_X}{m_{red} w^2} - \sqrt{1 - 2 \frac{\delta m_X}{m_{red} w^2}} \right), \frac{1}{2} m_X (u^2 + v(r_0)^2) - \delta m_X \right] \quad (17)$$

where the first term is the minimum recoil energy kinematically possible in two-body inelastic scattering, and the second term is the minimum recoil energy in a process where the outgoing dark matter particle is slower than v_e , the velocity to escape to radius r_0 .

u_{max} is determined by the constraint $E_{max} \geq E_{min}$, yielding

$$u_{max}^2 = \frac{1}{2} v^2 \frac{\mu}{\mu_-^2} \left[1 - \frac{2\delta m_X}{m_X v^2} \frac{\mu_-}{\mu} - \frac{(1 + \mu^2)v(r_0)^2}{2\mu v^2} + \sqrt{\left(1 - \frac{v(r_0)^2}{v^2} \right)^2 - 4 \frac{\delta m_X}{m_X} \frac{\mu_-}{v^2} \left(1 - \frac{v(r_0)^2}{v^2} \right)} \right]. \quad (18)$$

Finally, we have

$$u_{min}^2 = \max \left[\frac{2\delta m_X}{m_r} - v^2, 0 \right], \quad (19)$$

because inelastic scattering is only kinematically possible for $\delta m_X \leq (1/2)m_r w^2$. This implies that, for $m_X \lesssim 10$ GeV one need only consider models with $\delta m_X \lesssim \mathcal{O}(10 - 100)$ keV.

The capture rates for inelastic dark matter with contact interactions and $\delta m_X = 10, 30, 50$ keV are plotted in fig 4. It is interesting to note that, as δm_X increases, the rate of capture arising from scattering off light elements vanishes. This is because m_r is smallest for light elements, implying that they have the smallest maximum value of δm_X such that inelastic scattering is kinematically allowed. It is also worth noting that inelastic scattering for low-mass dark matter is kinematically allowed in the sun for larger δm_X than in the Earth, because dark matter within the sun has gained kinetic energy from gravitational infall. As a result, even low-mass inelastic dark matter with $\delta m_X \sim 50$ keV can be potentially probed by neutrino detectors.

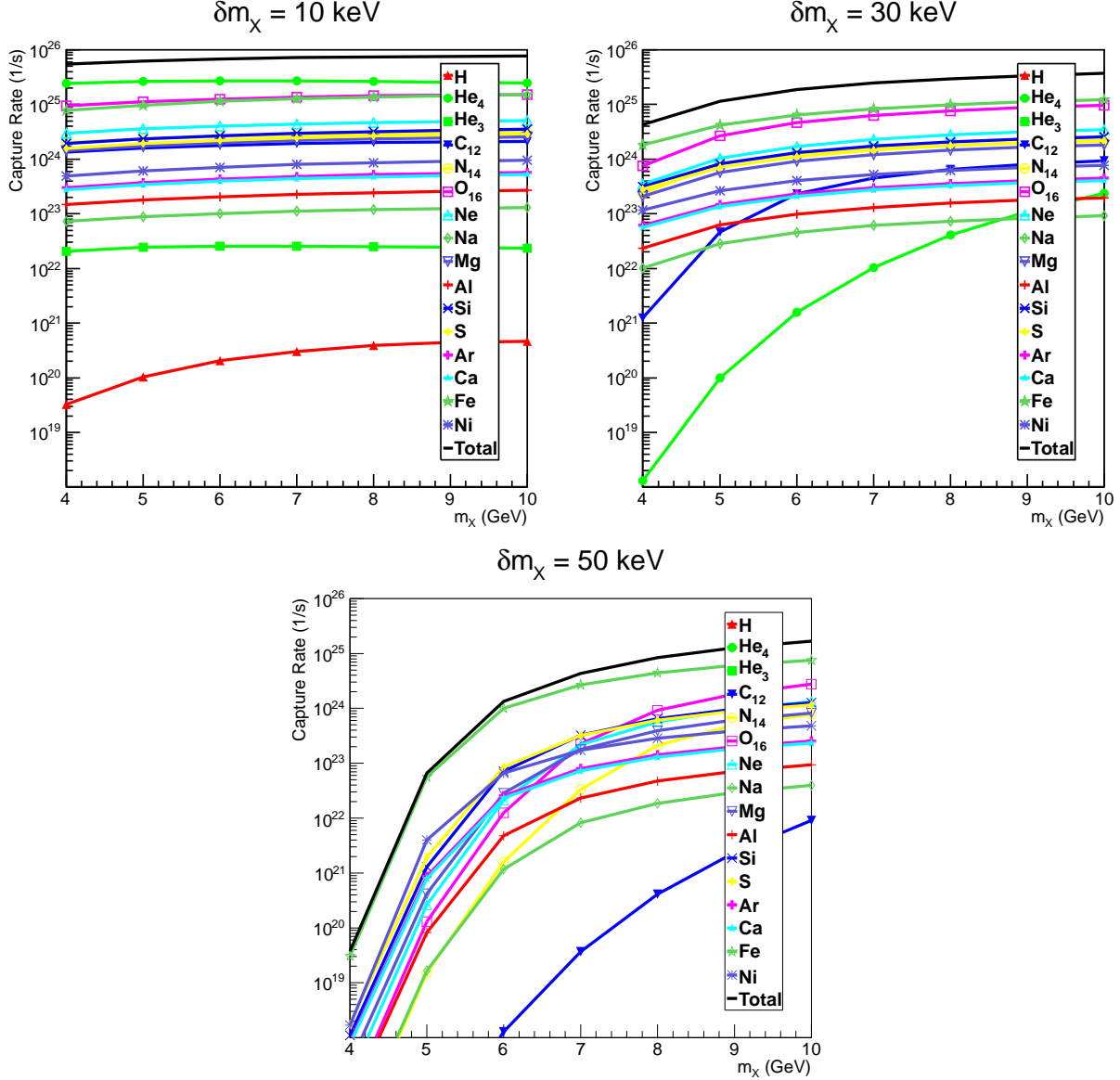


FIG. 4: Solar dark matter capture rates for various elements in the sun, assuming isospin-invariant inelastic elastic contact interactions with $I/32\pi = 10^{-4}$ pb GeV⁻². The three panels are for $\delta m_X = 10, 30$, and 50 keV, as labelled.

V. EQUILIBRIUM

If the effects of WIMP evaporation are negligible, the equilibration time τ_\odot for dark matter in the sun can be written as [54, 57]

$$\frac{t_\odot}{\tau_\odot} = 1.9 \times 10^{-11} \left(\frac{\Gamma_C^\odot}{\text{s}^{-1}} \right)^{\frac{1}{2}} \left(\frac{\langle \sigma v \rangle}{\text{pb}} \right)^{\frac{1}{2}} \left(\frac{m_X}{10 \text{ GeV}} \right)^{\frac{3}{4}}, \quad (20)$$

where $t_\odot \sim 4.5 \times 10^9$ yr is the age of the solar system.

For the case of elastic contact interactions (assumed to be isospin-invariant, and either spin-independent or spin-dependent), we plot in the top panel of fig. 5 the minimum σ^p

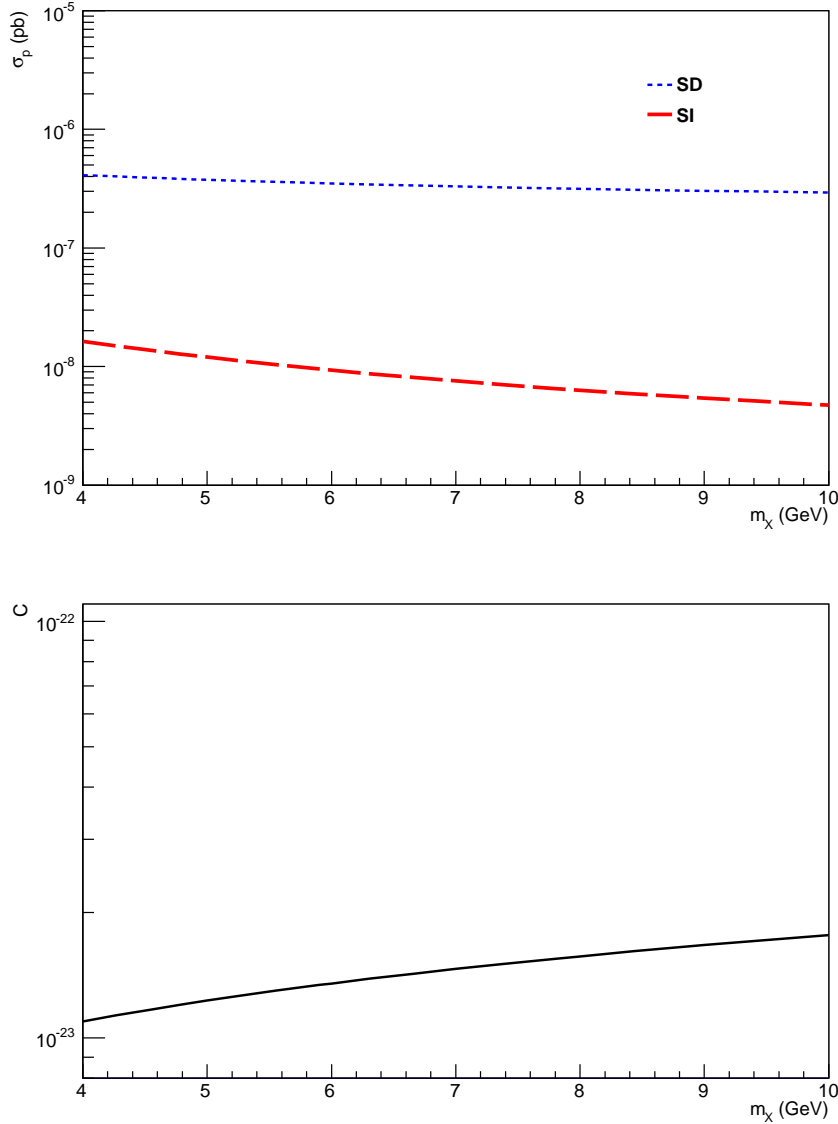


FIG. 5: Minimum σ^p (top panel) or C (bottom panel) required for dark matter to be in equilibrium in the sun, assuming either elastic contact (spin-dependent or spin-independent) or long-range interactions, respectively. We assume that the dark matter annihilation cross-section is given by $\langle\sigma v\rangle = 1$ pb.

required for the sun to currently be in equilibrium, assuming that the total dark matter annihilation cross-section is given by $\langle\sigma v\rangle = 1$ pb. Note that, for the case of IVDM with spin-independent interactions, the σ^p required for the sun to be in equilibrium would lie between that required for spin-dependent scattering and that required for isospin-invariant spin-independent scattering. Note that the equilibration time scales as $(\sigma^p\langle\sigma v\rangle)^{-1/2}$. IVDM with spin-independent interactions and $f_n/f_p \sim -0.7$ could be consistent with the data of DAMA, CoGeNT and XENON10/100 if $\sigma_{\text{SI}}^p \sim 10^{-2}$ pb [45, 46]. Such dark matter can be in equilibrium in the sun even if $\langle\sigma v\rangle \sim 10^{-5}$ pb. This implies that, if the IVDM candidate is a thermal relic, then it can currently be in equilibrium in the sun even if almost all of

the annihilation cross-section at freeze-out was due to p -wave interactions (suppressed at current times), with only a negligible amount due to s -wave interactions.

Similarly, for the case of long-range interactions, we plot in the bottom panel of fig. 5 the minimum C required for the sun to be in equilibrium (assuming $\langle\sigma v\rangle = 1$ pb).

VI. AN APPLICATION TO NEUTRINO DETECTORS

We now consider an application of these tools to a specific detector. We will focus on the case of long-range interactions, because neutrino detectors are expected to have a major advantage over direct detection experiments in this instance. For both direct detection experiments and neutrino searches, the measured event rate will be proportional to the dark matter-nucleus scattering cross-section. For the case of long-range interactions, the integrated dark matter-nucleus scattering cross-section is roughly proportional to $Cm_A^{-2}E_{min}^{-1}E_{max}^{-1}$, where m_A is the mass of the nucleus and E_{min} is the minimum nuclear recoil energy which one can measure. For a direct detection experiment, E_{min} is the recoil energy threshold of the experiment, and is typically of order $2 - 10$ keV. For germanium-based experiments (such as CDMS and CoGeNT), $m_A \sim 72 m_p$, while for xenon-based experiments $m_A \sim 130 m_p$. For neutrino searches, E_{min} is the minimum recoil energy such that dark matter is captured and can annihilate in the core of the sun. We thus find $E_{min} \approx (1/2)m_X u^2 \sim 2 - 5$ keV, for dark matter in the mass range considered here. However, m_A is the mass of the target nucleus in the sun and is very small for some elements that contribute significantly to capture in the sun. For example, hydrogen contributes $\sim 3\%$ of the dark matter capture rate for low-mass dark matter, and $m_H = m_p$. So one can expect the sensitivity of a neutrino search for low-mass dark matter with long range interactions to be significantly enhanced ($\sim 10^2 - 10^3$) compared to direct detection experiments.

We compare the sensitivity of liquid scintillation (LS) neutrino detectors to that of CDMS. It was shown in [58] that liquid scintillation neutrino-detectors can determine the flavor and direction of leptons produced by a charged-current interaction using the timing of the first photons which reach the photomultiplier tubes. We will focus on a search for electron neutrinos producing fully-contained electron/positron events. An advantage of this strategy is that the atmospheric electron neutrino background is significantly smaller than that of mu neutrinos. It was estimated that liquid scintillation neutrino detectors can provide almost absolute lepton flavor discrimination, and electrons of the energy range we consider can be measured with an angular resolution $\lesssim 1^\circ$. It was also estimated that the neutrino energy could be determined (from the energy and direction of the produced charged lepton, as well as total energy deposition) with a resolution $\sim 1 - 3\%$.

We will consider the sensitivity of a LS neutrino detector with a spherical fiducial volume $V_0 \sim 1000 \text{ m}^3$ and 2135 live-days of data (these are roughly the specifications of KamLAND). We estimate the neutrino detector's sensitivity utilizing the procedure outlined in section II. The density of the liquid scintillator is taken to be 80% that of water. Following [31], we define as "fully-contained" an electron/positron event starting within the detector with at least 10 radiation lengths (~ 4.3 m) contained within the detector. Furthermore, the lepton event must point back to the sun within a half-angle $\theta_{cone} = 20^\circ \sqrt{10 \text{ GeV}/E_\nu}$, and the energy of the neutrino must be obey $E_\nu \geq 1.5 \text{ GeV}$. We then find [31]

$$\int dV \eta(r) \times \epsilon(r, z) \sim \eta \times \frac{2}{3} \times \frac{1}{2} V_0, \quad (21)$$

where the factor $2/3$ is the fraction of lepton events which will be within θ_{cone} , and the factor $1/2$ is the fraction of the fiducial volume which will yield fully-contained events. It was shown in [31] that, using the background estimate of [59], one would expect less than 5 electron/positron events satisfying these cuts arising from atmospheric neutrinos during the specified runtime. We will thus consider a model which would produce 10 signal events arising from dark matter annihilating in the sun as being excludable.

To determine the electron (anti-)neutrino flux at Kamioka, we have used the WimpEvent routine, run on the Hawaii Open Supercomputing Center cluster. Of the 10^7 dark matter annihilations which were simulated (as described in section III) for each annihilation channel and value of m_X , 2×10^6 were used to compute the neutrino spectra at the detector. The effect of neutrino propagation through the earth typically suppresses $\langle Nz \rangle$ by $\sim 25 - 50\%$ (depending on the mass and the annihilation channel).

For CDMS, we will roughly estimate the sensitivity to dark matter with long-range interactions from their published bounds [7] on dark matter with elastic contact isospin-invariant interactions. The bound CDMS can place on C can be related to its bounds on σ_{SI}^p by the relation

$$C^{bound} = \sigma_{SI}^{p(bound)} \frac{m_{Ge}^2}{4\pi\alpha^2\mu_p^2} \frac{\int_{u_{min}}^{\infty} du [f(u)/u] w^2 E_{max}^{-1} \int_{E_{thr}}^{E_{max}} dE_R |F_{Ge}(E_R)|^2}{\int_{u_{min}}^{\infty} du [f(u)/u] w^2 E_{max}^{-1} \int_{E_{thr}}^{E_{max}} dE_R |F_{Ge}(E_R)|^2 / E_R^2}, \quad (22)$$

where u is the velocity of a dark matter particle far from the sun, and w is the velocity of the same particle once it has reached the surface of the earth. When it reaches the surface of the earth, the kinetic energy of the particle has increased by an amount equal to the change in the gravitational potential energy. The change in the gravitational potential energy due to the sun and the earth (V_{sun} and V_{earth} , respectively) can be written as $\Delta V_{sun,earth} = -(1/2)m_X v_{sun,earth}^2$, where $v_{sun} \approx 42.1$ km/s is the escape velocity of the sun at the radius of the earth's orbit, and $v_{earth} \approx 11.2$ km/s is the escape velocity of the earth at the surface of the earth. Using the relation $\Delta E_{kinetic} = -\Delta V_{sun} - \Delta V_{earth}$, we find $w = (u^2 + v_{sun}^2 + v_{earth}^2)^{1/2}$.

The maximum recoil energy which can be transferred to a germanium nucleus is $E_{max} = 2m_X^2 m_{Ge} w^2 / (m_X + m_{Ge})^2$. We assume a threshold energy $E_{thr} = 2$ keV [7]. u_{min} is the minimum dark matter velocity (far from the sun) such that scattering with $E_R > E_{thr}$ is kinematically possible, and is given by the expression $u_{min}^2 = \max[(m_{Ge} E_{thr} / 2m_r^2) - v_{sun}^2 - v_{earth}^2, 0]$.

We again assume a Gaussian form factor $F_A(E_R)$; for the recoil energy range of interest, the Gaussian form factor for germanium differs from the Helm form factor [60] by at most 6%. We will assume a Maxwell-Boltzmann velocity distribution with $\bar{v} = 270$ km/s, and that the galactic escape velocity is 600 km/s. We will also assume a constant efficiency for events with recoil energy greater than the threshold energy to appear in the CDMS low-energy analysis band. Due to this assumption, the result shown here should be regarded as only an estimate of the sensitivity CDMS could obtain with present data to dark matter models with long-range interactions.

The estimated sensitivity of CDMS and a 1 kT liquid scintillation neutrino detector are plotted in figure 6. For the LS neutrino detector, we assume 2135 live-days of data, and assume that dark matter annihilates exclusively to either $\tau\bar{\tau}$, $b\bar{b}$, $c\bar{c}$, $g\bar{g}$ or $\nu\bar{\nu}$ (with equal coupling to all three neutrino flavors). In [31], it was shown that the sensitivity of CDMS to 10 GeV dark matter with isospin-invariant elastic contact interactions is roughly an order of magnitude greater than that of a 1 kT LS detector. Our calculation of the relative

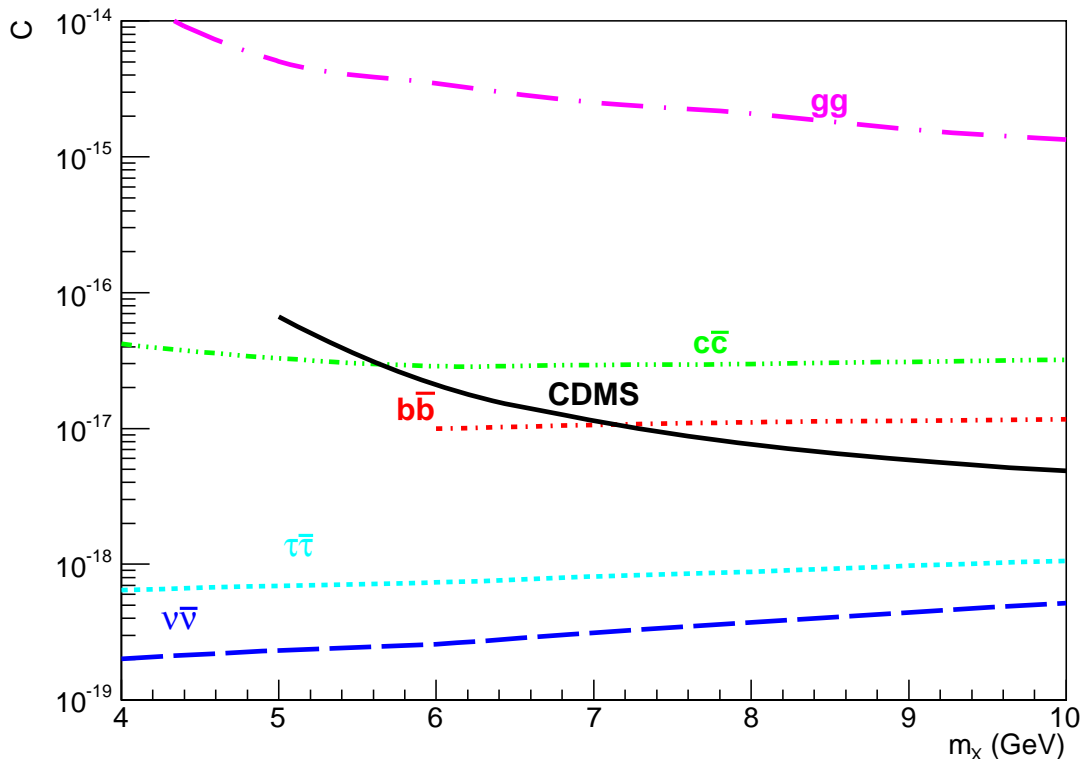


FIG. 6: Sensitivity to C of CDMS and a 1 kT LS detector (2135 live days of data) for low-mass dark matter with isospin-invariant elastic long-range interactions. LS detector sensitivity is shown assuming annihilation to either the τ , b , c , g and ν (flavor-independent) channels.

sensitivities of CDMS and a 1 kT LS detector to dark matter with long-range interactions bears out our original estimate of a roughly $10^2 - 10^3$ relative enhancement in sensitivity for the LS detector. Note that, for the models to which KamLAND would be sensitive, the sun would be in equilibrium (see figure 5) even if the annihilation cross-section were significantly smaller than 1 pb (assuming standard astrophysical assumptions). If the sun is not in equilibrium as a result of deviations from these assumptions, then the constraints which would be possible from neutrino detectors would be significantly suppressed.

We will not attempt a quantitative estimate of the sensitivity of XENON100 to dark matter with long-range interactions. XENON100's recoil energy threshold is defined in terms of scintillation photoelectrons; the detector's scintillation response to recoil energy (\mathcal{L}_{eff}) is not measured for low recoil energies. Moreover, bounds from XENON100 are generated assuming that the number of photoelectrons is determined by a Poisson distribution. Even some low energy recoils can thus produce enough scintillation photoelectrons to exceed the threshold. As a result of the uncertainties in the detector response at low recoil, an attempt to estimate the event rate expected at XENON100 for dark matter with long-range interactions is beyond the scope of this work. We will simply note that the recoil energy range for which XENON100 is sensitive is at best comparable to that of CDMS, while a xenon nucleus is roughly twice as heavy as that of germanium. This implies that the sensitivity of XENON100 relative to CDMS will be suppressed by roughly a factor of 4 for

the case of long-range interactions.

Recent hints of low-mass dark matter have potentially been seen by the DAMA [1], CoGeNT [2] and CRESST [3] experiments. Dark matter models with long-range interactions have been discussed as a possible way of reconciling the data from these experiments with the constraints from other direct detection experiments [61, 62]. Long-range interactions can affect not only the magnitude of the overall excesses seen by CoGeNT and CRESST, but can also affect the modulation seen by DAMA and CoGeNT. Although models with long-range interactions can provide a better fit to the overall excesses, they sometimes provide a worse fit to the modulation signals. We will not attempt to define a region of parameter-space for dark matter with long-range interactions which could match the DAMA, CoGeNT or CRESST data. This would require a detailed matching of the expected event spectrum with that observed by the experiments, which is beyond the scope of this work (and perhaps premature, given the issues raised in [15]). However, since CoGeNT also uses germanium as the target material, one would expect a 1 kT LS detector to be easily sensitive to dark matter models with long-range interactions which could potentially explain the data of CoGeNT. Moreover, one should note that the low-mass CRESST region is consistent with scattering from both oxygen and calcium. Given the difference in mass, one would expect long-range interactions with calcium to be suppressed by roughly a factor 4 relative to oxygen, as compared to the case of contact interactions.

Finally, we can consider the sensitivity of LBNE (Long-Baseline Neutrino Experiment). We will assume the detector target material is liquid argon (configuration 2) [63], with a total fiducial volume of roughly 51 kT. Liquid argon-based neutrino detectors are expected to have very good event reconstruction; we will assume that liquid argon detectors permit a reconstruction of charged lepton flavor, energy and direction with at least the same resolution as liquid scintillation detectors. We then find

$$\int dV \eta(r) \times \epsilon(r, z) \sim \frac{2}{3} \times (3.1 \times 10^{34}) \quad (23)$$

where the factor $2/3$ again arises from the fraction of charged lepton events which would point back to the sun within angle θ_{cone} . For a detector as large as LBNE, almost the entire fiducial volume can produce fully-contained events. We then see that the sensitivity which KamLAND could obtain with its 2135 day data set could be obtained by LBNE with only ~ 17 days of data.

Note that the possibility of dominant annihilation to leptonic channels is not inconsistent with dark matter-nucleus scattering which is large enough to be probed by neutrino detectors. For example, it could be that dark matter-quark scattering is mediated by an effective operator which permits velocity-independent, spin-independent scattering, but does not permit s -wave annihilation (an example of such an operator is $\bar{X}X\bar{q}q$). In this case, the dark matter-nucleus scattering cross-section could be reasonably large, while the cross-section for dark matter to annihilate to quarks would be v^2 -suppressed. If dark matter coupled to leptons through an operator which permitted s -wave annihilation (an example of such an operator would be $\bar{X}\gamma_\mu X\bar{f}\gamma^\mu f$, if the dark matter were a Dirac fermion), then the dark matter would mostly annihilate to leptons.

VII. CONCLUSIONS

We have computed the capture rates and neutrino spectra which are relevant for neutrino-based searches for low-mass dark matter in the sun. The neutrino spectra are presented at a distance of 1 AU from the sun, accounting for matter effects in the sun, and vacuum oscillations (assuming a normal hierarchy and $\theta_{13} = 10^\circ$). The capture rates have been found assuming either elastic contact, elastic long-range, or inelastic contact interactions. These are the tools required for a neutrino detector to search for dark matter annihilating in the sun.

As an application of these tools, we plot the sensitivity of a 1 kT LS detector, with 2135 days of data, to low-mass dark matter with isospin-invariant elastic long-range interactions with Standard Model nucleons. We have found that neutrino detectors have a greatly enhanced sensitivity to dark matter with long-range interactions, relative to leading direct detection experiments such as CDMS. This enhancement is readily understood; in the case of long-range interactions, the scattering matrix element is inversely proportional to $q^2 = 2m_A E_R$. Scattering rates in detectors with heavy targets, such as germanium and xenon, are heavily suppressed. Dark matter capture in the sun involves scattering from low-mass targets such as hydrogen and helium, implying that these scattering rates will see a relative enhancement. A LS neutrino detector with the exposure already available to KamLAND could have a sensitivity up to 2 orders of magnitude greater than that of CDMS. LBNE (with a 51 kT liquid argon target) could achieve similar sensitivity with roughly 17 days of data.

We have also found that low-mass dark matter with inelastic contact interactions can be probed by neutrino detectors even for $\delta m_X \sim 50$ keV. This implies that neutrino detectors can be sensitive to inelastic dark matter models which are more difficult to probe on earth, because gravitational infall allows inelastic scattering in the sun for models where inelastic scattering would not be kinematically possible on earth.

The choice $\theta_{13} = 10^\circ$ is consistent with recent data from the Daya Bay experiment [53]. The neutrino spectrum is slightly different from the $\theta_{13} = 0^\circ$ case, with the difference most noticeable in the case of annihilation entirely to neutrinos. For searches involving upward-going leptons, there will also be a modification to the neutrino spectrum due to passage through the earth. This effect will depend on the location of the detector; for any particular detector, one can obtain the appropriate neutrino spectra by running the WimpEvent program, inputting the data files for the neutrino spectrum at 1 AU found at <http://www.phys.hawaii.edu/~superk/post/spectrum>.

It is worth noting that a direct detection experiment with a target molecule containing hydrogen would also be expected to have enhanced sensitivity to dark matter with long-range interactions. Gaseous time projection chambers (such as DRIFT [64], DMTPC [65], D^3 [66], MIMAC [67] and NEWAGE [68]) using hydrocarbon targets may be well-suited for this type of search.

Specific dark matter models with long-range interactions may have solar capture rates that are enhanced by collective effects, such as multiple scattering. Neutrino searches thus have enhanced sensitivity to such models, and current data may already provide tight constraints. It would be interesting to consider such models in more detail.

VIII. ACKNOWLEDGMENTS

We gratefully acknowledge K. Choi, D. Marfatia, M. Sakai, P. Subramoney and S. Vahsen for useful discussions. We also thank the Hawaii Open Supercomputing Center. This work is supported in part by the Department of Energy under Grant DE-FG02-04ER41291.

Appendix A: Neutrino Spectra

In this appendix, we plot the neutrino and anti-neutrino spectra at a distance 1 AU from the sun, assuming dark matter annihilation exclusively to either the $b\bar{b}$ or $\tau\bar{\tau}$ channels. Each spectrum was generated by simulating 10^7 annihilations using the method described in the text. Here, $z \equiv E_\nu/m_X$, and neutrino oscillations are generated assuming $\theta_{13} = 10^\circ$.

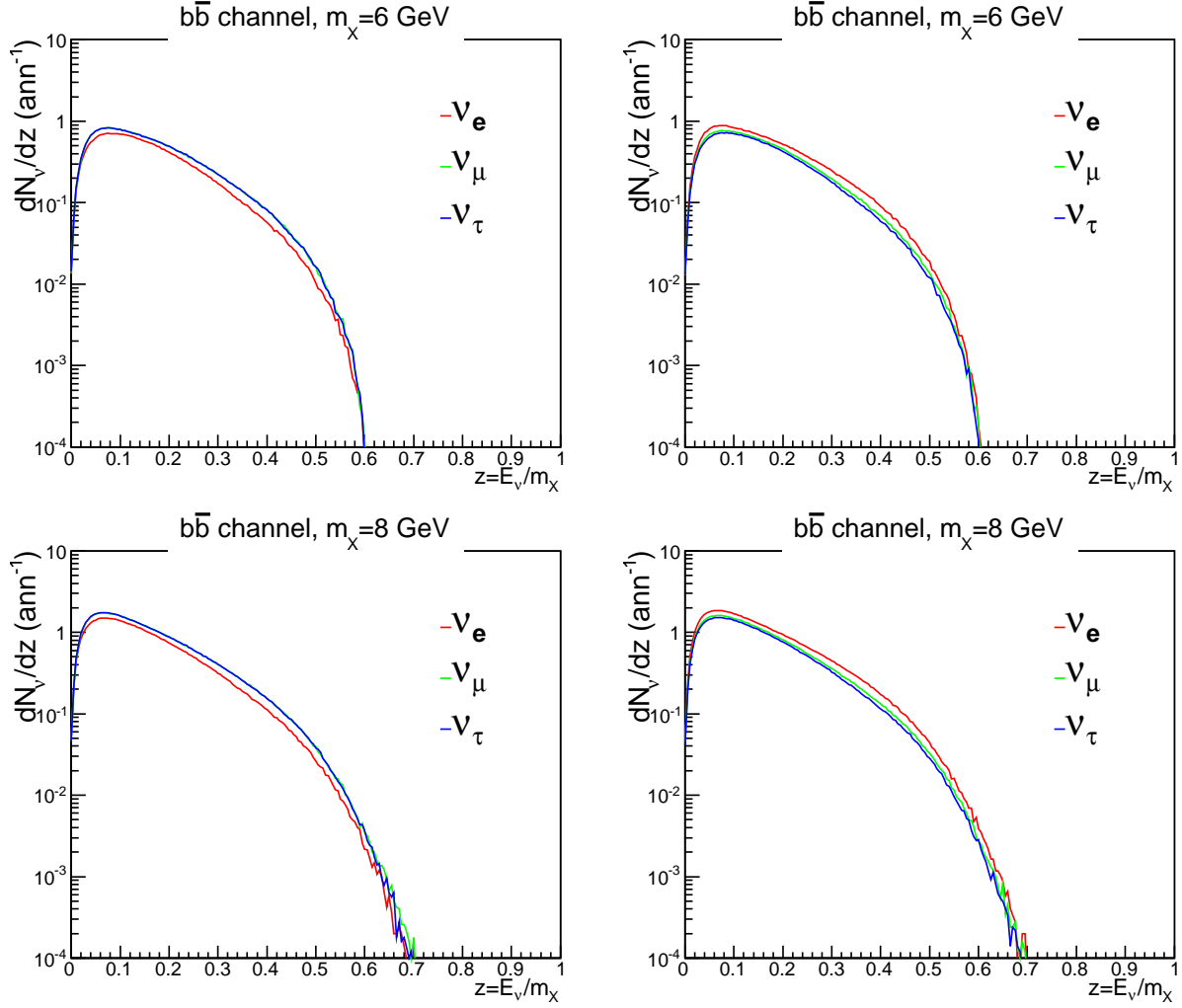


FIG. 7: Neutrino spectra (left panels) and anti-neutrino spectra (right panels) at 1 AU for dark matter annihilation to the $b\bar{b}$ channel. The spectra for ν_e ($\bar{\nu}_e$), ν_μ ($\bar{\nu}_\mu$), and ν_τ ($\bar{\nu}_\tau$) are shown in red, green, and blue, respectively. Spectra are shown for $m_X = 6, 8$ GeV.

-
- [1] R. Bernabei, *et al.*, Eur. Phys. J. **C67**, 39-49 (2010). [arXiv:1002.1028 [astro-ph.GA]]; P. Belli, R. Bernabei, A. Bottino, F. Cappella, R. Cerulli, N. Fornengo and S. Scopel, Phys. Rev. D **84**, 055014 (2011) [arXiv:1106.4667 [hep-ph]].
 - [2] C. E. Aalseth, *et al.*, Phys. Rev. Lett. **107**, 141301 (2011). [arXiv:1106.0650 [astro-ph.CO]].
 - [3] G. Angloher, *et al.*, [arXiv:1109.0702 [astro-ph.CO]].
 - [4] J. Angle *et al.*, Phys. Rev. Lett. **107**, 051301 (2011). [arXiv:1104.3088 [astro-ph.CO]].
 - [5] E. Aprile *et al.*, Phys. Rev. Lett. **107**, 131302 (2011). [arXiv:1104.2549 [astro-ph.CO]].
 - [6] D. S. Akerib *et al.*, Phys. Rev. D **82**, 122004 (2010) [arXiv:1010.4290 [astro-ph.CO]].
 - [7] Z. Ahmed *et al.*, Phys. Rev. Lett. **106**, 131302 (2011). [arXiv:1011.2482 [astro-ph.CO]].
 - [8] Z. Ahmed *et al.* [CDMS Collaboration], arXiv:1203.1309 [astro-ph.CO].
 - [9] J. I. Collar and D. N. McKinsey, arXiv:1005.0838 [astro-ph.CO].

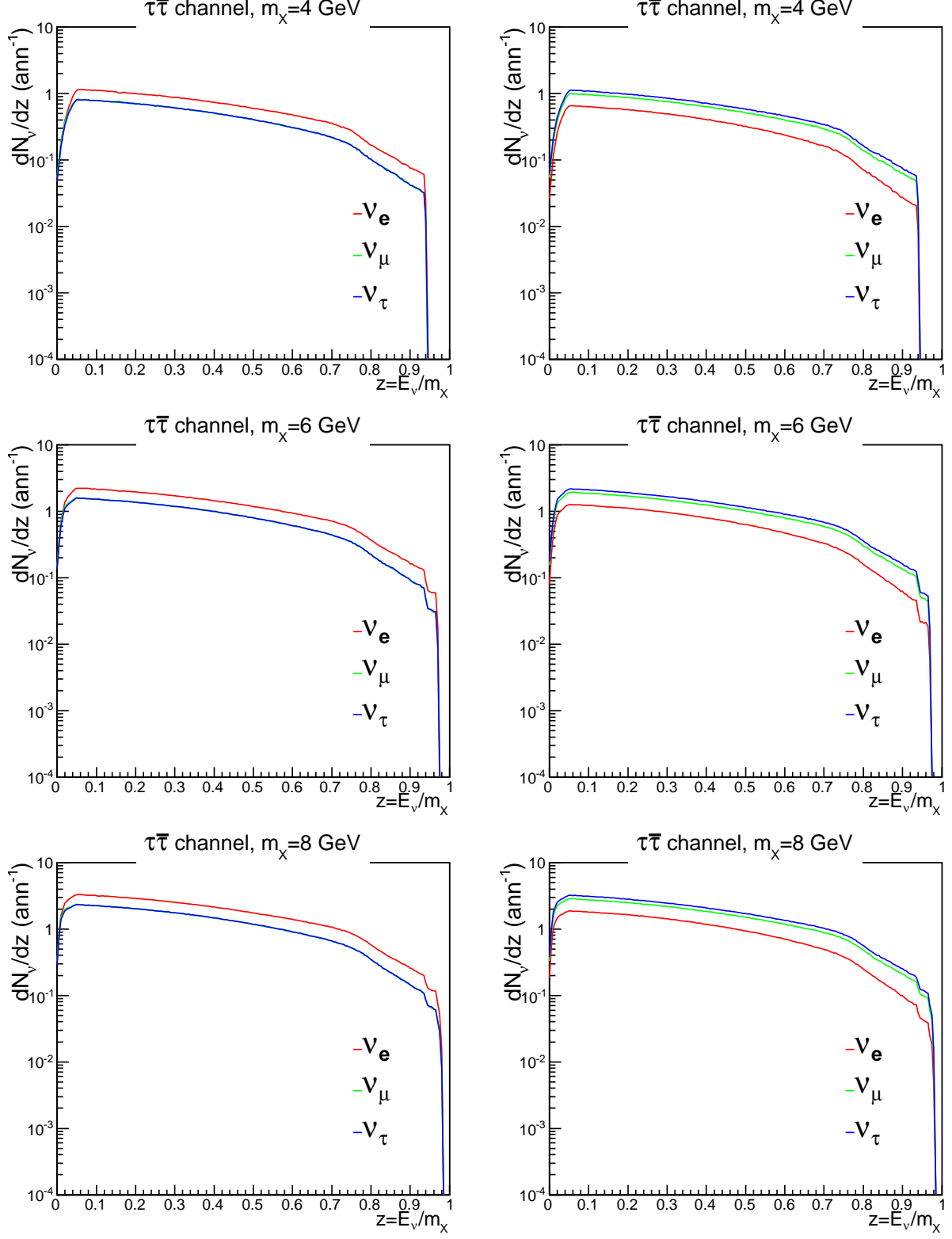


FIG. 8: Neutrino spectra (left panels) and anti-neutrino spectra (right panels) at 1 AU for dark matter annihilation to the $\tau\bar{\tau}$ channel. The spectra for $\nu_e(\bar{\nu}_e)$, $\nu_\mu(\bar{\nu}_\mu)$, and $\nu_\tau(\bar{\nu}_\tau)$ are shown in red, green, and blue, respectively. Spectra are shown for $m_X = 4, 6, 8$ GeV.

- [10] The XENON100 Collaboration, arXiv:1005.2615 [astro-ph.CO].
- [11] J. I. Collar and D. N. McKinsey, arXiv:1005.3723 [astro-ph.CO].
- [12] J. I. Collar, arXiv:1010.5187 [astro-ph.IM].
- [13] J. I. Collar, arXiv:1103.3481 [astro-ph.CO].
- [14] J. I. Collar, arXiv:1106.0653 [astro-ph.CO].
- [15] Talk by J. Collar, TAUP 2011 Workshop, Munich, Germany, Sep. 5-9, 2011.
- [16] M. Kuzniak, M. G. Boulay and T. Pollmann, arXiv:1203.1576 [astro-ph.IM].
- [17] J. I. Collar and N. E. Fields, arXiv:1204.3559 [astro-ph.CO].
- [18] Q. -H. Cao, I. Low and G. Shaughnessy, Phys. Lett. B **691**, 73 (2010) [arXiv:0912.4510 [hep-ph]].
- [19] J. Goodman, *et al.*, Phys. Lett. **B695**, 185-188 (2011). [arXiv:1005.1286 [hep-ph]].
- [20] J. Lavalle, Phys. Rev. D **82**, 081302 (2010) [arXiv:1007.5253 [astro-ph.HE]].
- [21] J. Goodman, *et al.*, Phys. Rev. **D82**, 116010 (2010). [arXiv:1008.1783 [hep-ph]].
- [22] A. Rajaraman, *et al.*, [arXiv:1108.1196 [hep-ph]].
- [23] R. Kappl and M. W. Winkler, arXiv:1110.4376 [hep-ph].
- [24] J. Goodman and W. Shepherd, arXiv:1111.2359 [hep-ph].
- [25] A. Friedland, M. L. Graesser, I. M. Shoemaker and L. Vecchi, arXiv:1111.5331 [hep-ph].
- [26] J. Kumar, D. Sanford and L. E. Strigari, arXiv:1112.4849 [astro-ph.CO].
- [27] I. M. Shoemaker and L. Vecchi, arXiv:1112.5457 [hep-ph].
- [28] D. Hooper, F. Petriello, K. M. Zurek and M. Kamionkowski, Phys. Rev. D **79**, 015010 (2009) [arXiv:0808.2464 [hep-ph]].
- [29] J. L. Feng, J. Kumar, J. Learned and L. E. Strigari, JCAP **0901**, 032 (2009) [arXiv:0808.4151 [hep-ph]].
- [30] A. L. Fitzpatrick, D. Hooper and K. M. Zurek, Phys. Rev. D **81**, 115005 (2010) [arXiv:1003.0014 [hep-ph]].
- [31] J. Kumar, J. G. Learned, M. Sakai and S. Smith, Phys. Rev. D **84**, 036007 (2011) [arXiv:1103.3270 [hep-ph]].
- [32] S. -L. Chen and Y. Zhang, Phys. Rev. D **84**, 031301 (2011) [arXiv:1106.4044 [hep-ph]].
- [33] S. K. Agarwalla, M. Blennow, E. F. Martinez and O. Mena, JCAP **1109**, 004 (2011) [arXiv:1105.4077 [hep-ph]].
- [34] A. Gould, Astrophys. J. **321**, 560 (1987); K. Griest and D. Seckel, Nucl. Phys. B **283**, 681 (1987) [Erratum-ibid. B **296**, 1034 (1988)]; M. Kamionkowski *et al.* Phys. Rev. Lett. **74**, 5174 (1995) [arXiv:hep-ph/9412213].
- [35] P. Gondolo, J. Edsjo, P. Ullio, L. Bergstrom, M. Schelke and E. A. Baltz, JCAP **0407**, 008 (2004) [astro-ph/0406204].
- [36] R. Foot, Phys. Lett. B **703**, 7 (2011) [arXiv:1106.2688 [hep-ph]].
- [37] N. Fornengo, P. Panci and M. Regis, Phys. Rev. D **84**, 115002 (2011) [arXiv:1108.4661 [hep-ph]].
- [38] R. Foot, arXiv:1203.2387 [hep-ph].
- [39] M. T. Frandsen, *et al.*, Phys. Rev. D **84**, 041301 (2011) [arXiv:1105.3734 [hep-ph]].
- [40] D. Tucker-Smith and N. Weiner, Phys. Rev. D **64**, 043502 (2001) [hep-ph/0101138].
- [41] D. Tucker-Smith and N. Weiner, Phys. Rev. D **72**, 063509 (2005) [hep-ph/0402065].
- [42] S. Chang, G. D. Kribs, D. Tucker-Smith and N. Weiner, Phys. Rev. D **79**, 043513 (2009) [arXiv:0807.2250 [hep-ph]].
- [43] K. Schmidt-Hoberg and M. W. Winkler, JCAP **0909**, 010 (2009) [arXiv:0907.3940 [astro-ph.CO]].

- [44] J. M. Cline, A. R. Frey and F. Chen, Phys. Rev. D **83**, 083511 (2011) [arXiv:1008.1784 [hep-ph]].
- [45] S. Chang, J. Liu, A. Pierce, N. Weiner and I. Yavin, JCAP **1008**, 018 (2010) [arXiv:1004.0697 [hep-ph]].
- [46] J. L. Feng, J. Kumar, D. Marfatia and D. Sanford, Phys. Lett. B **703**, 124 (2011) [arXiv:1102.4331 [hep-ph]].
- [47] J. M. Cline and A. R. Frey, Phys. Rev. D **84**, 075003 (2011) [arXiv:1108.1391 [hep-ph]]; J. M. Cline and A. R. Frey, arXiv:1109.4639 [hep-ph].
- [48] J. Edsjo, TSL-ISV-93-0091.
- [49] G. Jungman and M. Kamionkowski, “Neutrinos from particle decay in the sun and earth,” Phys. Rev. D **51**, 328 (1995) [arXiv:hep-ph/9407351]; M. Blennow, J. Edsjo and T. Ohlsson, “Neutrinos from WIMP Annihilations Using a Full Three-Flavor Monte Carlo,” JCAP **0801**, 021 (2008) [arXiv:0709.3898 [hep-ph]].
- [50] C. Rott, J. Siegal-Gaskins and J. F. Beacom, arXiv:1208.0827 [astro-ph.HE].
- [51] J. Edsjo, WimpSim Neutrino Monte Carlo, <http://www.physto.se/~edsjo/wimpsim/>
- [52] T. Sjostrand, S. Mrenna and P. Z. Skands, JHEP **0605**, 026 (2006) [hep-ph/0603175].
- [53] F. P. An *et al.* [DAYA-BAY Collaboration], arXiv:1203.1669 [hep-ex].
- [54] G. Jungman, M. Kamionkowski, K. Griest, “Supersymmetric dark matter,” Phys. Rept. **267**, 195-373 (1996). [hep-ph/9506380].
- [55] V. Barger, Y. Gao and D. Marfatia, Phys. Rev. D **83**, 055012 (2011) [arXiv:1101.4410 [hep-ph]].
- [56] A. Gould, “Resonant Enhancements in WIMP Capture by the Earth,” Astrophys. J. **321**, 571 (1987).
- [57] K. Griest and D. Seckel, Nucl. Phys. B **283**, 681 (1987) [Erratum-ibid. B **296**, 1034 (1988)].
- [58] J. G. Learned, arXiv:0902.4009 [hep-ex]; J. Peltoniemi, [arXiv:0909.4974 [physics.ins-det]].
- [59] M. Honda, T. Kajita, K. Kasahara and S. Midorikawa, arXiv:1102.2688 [astro-ph.HE].
- [60] J. D. Lewin and P. F. Smith, Astropart. Phys. **6**, 87 (1996); G. Duda, A. Kemper and P. Gondolo, JCAP **0704**, 012 (2007) [hep-ph/0608035].
- [61] T. Schwetz and J. Zupan, JCAP **1108**, 008 (2011) [arXiv:1106.6241 [hep-ph]]; M. Farina, D. Pappadopulo, A. Strumia and T. Volansky, JCAP **1111**, 010 (2011) [arXiv:1107.0715 [hep-ph]]; N. Fornengo, P. Panci and M. Regis, Phys. Rev. D **84**, 115002 (2011) [arXiv:1108.4661 [hep-ph]].
- [62] R. Foot, arXiv:1203.2387 [hep-ph].
- [63] T. Akiri *et al.* [LBNE Collaboration], arXiv:1110.6249 [hep-ex].
- [64] E. Daw, A. Dorofeev, J. R. Fox, J. -L. Gauvreau, C. Ghag, L. J. Harmon, J. L. Harton and M. Gold *et al.*, arXiv:1110.0222 [physics.ins-det].
- [65] J. Monroe, for the DMTPC Collaboration, arXiv:1111.0220 [physics.ins-det].
- [66] S. E. Vahsen, H. Feng, M. Garcia-Sciveres, I. Jaegle, J. Kadyk, Y. Nguyen, M. Rosen and S. Ross *et al.*, arXiv:1110.3401 [astro-ph.IM].
- [67] D. Santos, J. Billard, G. Bosson, J. L. Bouly, O. Bourrion, C. Fourel, O. Guillaudin and F. Mayet *et al.*, arXiv:1111.1566 [astro-ph.IM].
- [68] K. Miuchi, H. Nishimura, K. Hattori, N. Higashi, C. Ida, S. Iwaki, S. Kabuki and H. Kubo *et al.*, Phys. Lett. B **686**, 11 (2010) [arXiv:1002.1794 [astro-ph.CO]].